PERGAMON

International Journal of Impact Engineering 26 (2001) 603–611

INTERNATIONAL JOURNAL OF IMPACT ENGINEERING

www.elsevier.com/locate/ijimpeng

HYPERVELOCITY JACKETED PENETRATORS

BRADLEY A. PEDERSEN, STEPHAN J. BLESS, and JAMES U. CAZAMIAS

Institute for Advanced Technology, The University of Texas at Austin, 3925 W. Braker Lane, Suite 400, Austin, TX 78759-5316

Abstract—The use of steel jackets was found to significantly improve the penetration efficiency of tungsten alloy rods. Experiments and analyses were conducted with L/D=10 projectiles of constant exterior dimensions at a nominal impact velocity of 2.2 km/s. The fraction of jacket material was varied to see which geometry would have the best performance. For a core-to-jacket diameter ratio (μ) of 0.6, the experiments showed the penetration efficiency ($P/KE^{1/3}$) increased by 21% relative to an all-tungsten baseline rod of the same exterior dimensions. Experiments and AUTODYN simulations showed the same penetration efficiency trends. The simulations, however, did not show that the tungsten core outran the jacket, contrary to what was observed in the experiments.

BACKGROUND

The use of jackets effectively increases the length-to-diameter ratio (L/D) of rod projectiles. Improved stiffness from the jacket, which aids in launch and flight, and the effect of jackets on penetration have been previously examined. Sorensen, *et al.* [1] showed through analyses and numerical calculation that steel jacketed depleted uranium penetrators, at a velocity of 1.7 km/s, displayed no penetration degradation for jackets of diameter ratios down to 0.8. Lehr, *et al.* [2], using carbon fiber jacketed tungsten penetrators, found penetration depth in semi-infinite RHA was handicapped at velocities less than 2.2 km/s but showed no degradation between 2.3 and 2.5 km/s. In their experiments, the jacket failed to penetrate deeper than a few crater diameters, even at 2.5 km/s. Lanz and Lehr [3] showed the benefits of using steel jackets on tungsten rods against complex armors. The jacketed penetrators did not break up as much as rods when tested against spaced, oblique plates. The present study evaluates the effect of steel jackets on tungsten rods penetrating monolithic steel targets at a nominal velocity of 2.2 km/s.

NUMERICAL STUDIES

Computations were initially performed to investigate jacket effects and to help design experiments. The two-dimensional Eulerian version of AUTODYN was used with axial symmetry. Gridding was relatively fine, with five cells per millimeter. All materials were modeled as elastic-plastic. In one simulation, a row of void cells was placed between the jacket and core in order to investigate mixed cell effects. In another, the steel jacket strength was increased to 1.3 GPa. In neither case did the results differ significantly from the baseline simulations. Table 1 shows the material properties used in the simulations.

0734-743X/01/$ - see front matter
PII: S0734-743X(01)00121-X

Table 1. Material properties from computations

Material	Density, g/cc	Yield Stress, GPa
Jacket - 1006 Steel	7.896	0.35
Core - Tungsten	17.4	2.2
Target - RHA	7.860	1.5

Table 2 lists the geometries and penetration results from the computations. The value of μ is defined as the core-to-jacket diameter ratio (D_c/D_j). A μ value of 1 implies an all-tungsten rod, while a 0 value is an all-steel rod. Jacket thickness is also shown in the table. The penetration depth is the deepest for the all-tungsten rod, but the penetration efficiency is the highest for the μ=0.6 jacket. Computed as the penetration depth divided by the cube root of the kinetic energy ($P/KE^{1/3}$), this parameter gives the relative penetration of equal energy projectiles. This parameter is scale independent to the extent that penetration normalized by length (P/L) is scale independent.

Table 2. AUTODYN simulation penetrator geometries and results

Simulation	μ	Core D, mm	Jacket D, mm	Jacket t, mm	L, mm	L/D	P, mm	P/KE^1/3
1	1	10	0	-	100	10	121	1.75
2	0.8	8	10	1	100	10	117	1.82
3	0.6	6	10	2	100	10	110	1.84
4	0.4	4	10	3	100	10	96	1.71
5	0.2	2	10	4	100	10	77	1.43
6	0	0	10	5	100	10	57	1.07

Penetration channel contours are plotted in Figure 1. As more of the tungsten is replaced with steel (thicker and thicker jackets), the ultimate penetration depth suffers. The crater diameter remains essentially constant between simulations. In all simulations, the entire rod penetrates in unison, as seen in Figure 2. The jacket material was turned around inside the tungsten mushroom head. In this figure, the penetrator has been penetrating for approximately 48 μs.

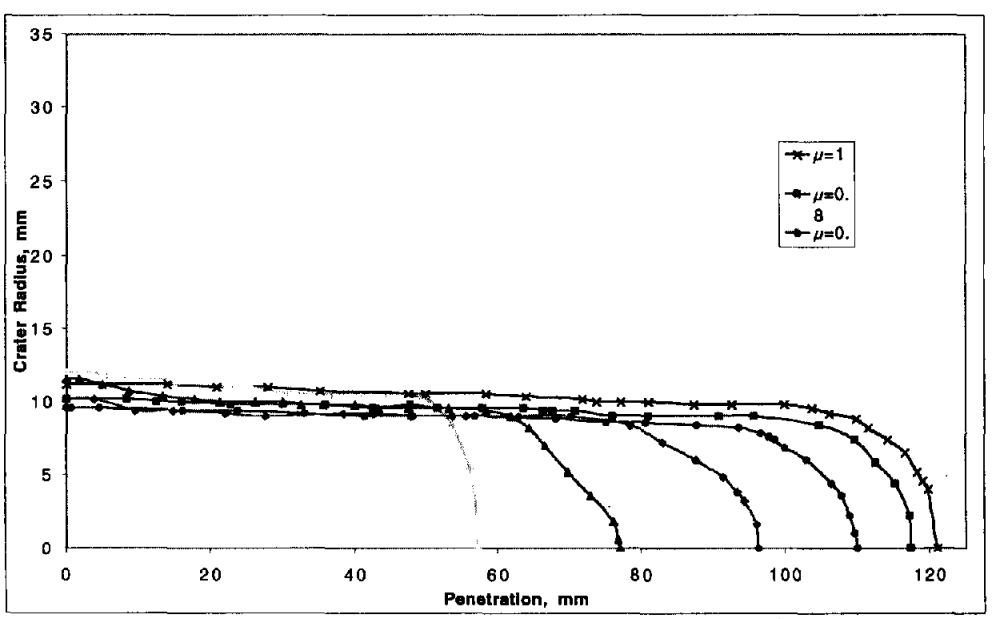

Fig. 1. Penetration channels from AUTODYN simulations.

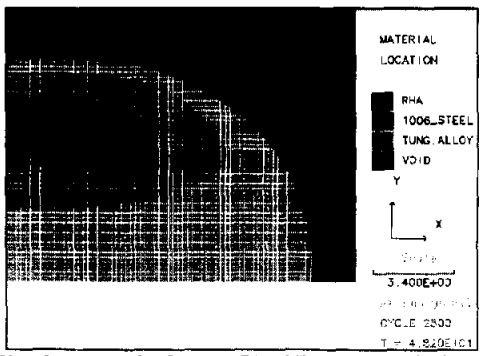

Fig. 2. Sample from AUTODYN simulations.

The simulations were also used to see if the jacket and core had the same velocities. Figure 3 shows the tail velocities of the cores and jackets as a function of time from each of the simulations. In general, the cores and jackets decelerate at the same rate until the end of the penetration event, when the jackets decelerate more rapidly. This can be seen in the figure by the slightly steeper slope of the dashed-line, open symbol, jacket velocity curves. These results imply that the cores and jackets were penetrating together.

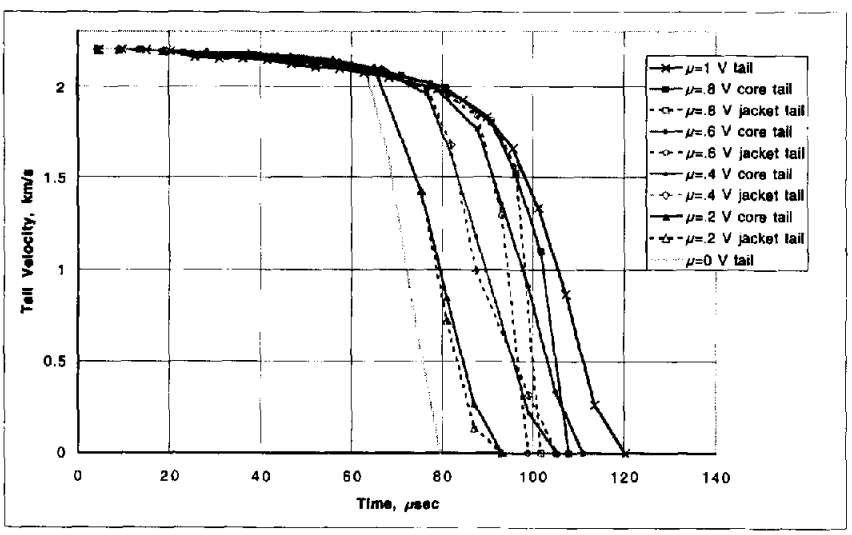

Fig. 3. Tail velocity from AUTODYN simulations.

EXPERIMENTAL RESULTS

Based on the numerical predictions, jacketed rods with μ values of 0.6 and 0.4 were tested along with an all-tungsten, equivalent exterior dimension, baseline rod. These two geometries were chosen because they provided good efficiency, as shown in the simulations. An all-tungsten rod was tested to provide a reference penetration value. Exterior dimensions were maintained constant with a length of 100mm and a diameter of 10mm. The core rod was a 91% tungsten alloy with nickel and cobalt alloying elements. The density of this alloy is 17.45 g/cm^3. The jacket material was 4130 steel, heat-treated to a hardness of 352 BHN. Jackets were attached to the cores with epoxy. Projectiles were launched in base-pushed, discarding petal sabots from a 115/38 mm two stage light gas gun at the IAT. Figure 4 shows a disassembled launch package. The sabot is made of four interlocking plastic petals, a titanium pusher plate,

and a plastic obturator. Table 3 lists the dimensions of the penetrator geometries tested. Notice that the exterior penetrator dimensions were kept constant rather than the mass. Targets were semi-infinite RHA with a hardness in the range of 300-330 BHN.

Fig. 4. L/D 10 penetrator and launch package.

Table 3. Penetrator dimensions from IAT testing

IAT Test	Diameter Ratio, mu	Jacket Diameter, mm	Core Diameter, mm	Rod Length, mm	L/D	Mass, g
450	0.6	10	6	100	10	87
453	0.4	10	4	100	10	73
454	0.6	10	6	100	10	88
465	1	0	10	99.6	10	137

Test results are listed in Table 4, including impact velocity, yaw, ultimate penetration, and the penetration as a function of length (P/L). Although some projectiles impacted with yaw, the total yaw was still below the critical value at which interference with the crater walls occurs. Silsby [4] developed an empirical relation for this as a function of penetrator L/D and velocity. This relation was applied to these tests to insure that impact yaw was below the critical value in each test. As can be seen, the penetration from the μ=0.6 diameter ratio rods was as deep as the all-tungsten baseline rod. This implies that adding a relatively thick steel jacket around a tungsten core does not inhibit the penetration depth into RHA.

Table 4. IAT testing results

IAT Test	Test Velocity, km/s	Pitch, deg	Yaw, deg	Pen Depth, mm	P/L
450	2.17	0.1	-0.7	142.6	1.43
453	2.16	-0.6	2.3	118.1	1.18
454	2.23	-2.2	-2.5	147	1.47
465	2.32	-2.3	-3.9	144	1.44

AVERAGE DENSITY PENETRATION FUNCTION

In order to clarify the effects of jacket construction, an analysis was conducted of homogeneous rods having the same density as the jacketed rods. For this purpose, a model was created for penetration as a function of density. The model was based on the Lanz-Odermatt [5] penetration function (Equation 1). A linear interpolation was used to vary the a and b parameters (Equations 2 and 3, respectively) between the values for the all-steel and all-tungsten penetrators.

$$\frac{P}{L} = a\exp\left[-\left(\frac{b}{V}\right)^2\right] \tag{1}$$

$$a = a_o\left[1 + n\left(\frac{\rho_o - \rho_{avg}}{\rho_t}\right)\right]\sqrt{\frac{\rho_{avg}}{\rho_o}} \tag{2}$$

$$b = b_o\left[1 + m\left(\frac{\rho_o - \rho_{avg}}{\rho_t}\right)\right]\sqrt{\frac{\rho_o}{\rho_{avg}}} \tag{3}$$

where,

ρ_o	tungsten density
ρ_t	target density
ρ_{avg}	average density
a_o, b_o	empirical values for tungsten data
n, m	interpolation parameters

The all-steel penetrator a and b parameters were determined by fitting data of Hohler and Stilp [6] for L/D=10 steel penetrators of hardnesses 230-540 BHN tested against armor steel of hardnesses 255-295 BHN. The parameters a and b (for all-steel rods) were 1.271 and 1.718 km/s, respectively. Values of a_o and b_o for the all-tungsten penetrator were found from Hohler and Stilp L/D=10 tungsten data [6], shown in Figure 5. It should be noted that the baseline, all-tungsten rod that was tested at IAT had a P/L value higher than would be predicted from Figure 5. As seen previously in Table 4, the all-tungsten rod (Test #465) had a P/L of 1.44. From Figure 5, one would find a value of approximately 1.3 for P/L which is approximately 10% less than seen in the experiment.

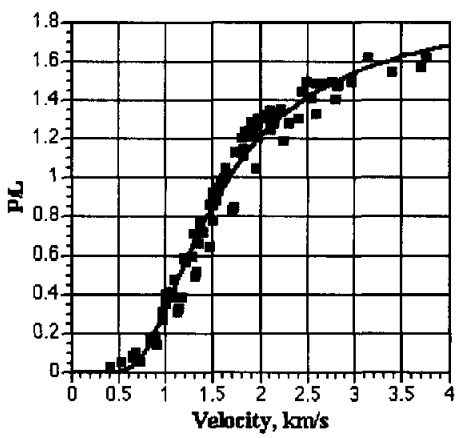

Fig. 5. Tungsten penetration normalized by length into armor steel.

To find a and b as functions of average density, the interpolation parameters n and m were varied until Equations 2 and 3 yielded the a and b values for an all-steel penetrator. The interpolation parameters were found to be n=0.046 and m=-0.087. Once the parameters a and b were known as a function of average density, P/L could also be found as a function of average density. As expected using the model, as μ decreases (smaller tungsten core), the P/L also decreases. This is the expected result since the model assumes a homogenized penetrator with an average density. Since the average density is lower than the density of tungsten, the jacketed rods do not perform as well. Figure 6 shows P/L as a function of velocity for several diameter

ratios. This figure shows that according to the average density penetration model, adding a jacket always decreases penetration efficiency. This contradicts the test data. As evident in the testing, the tungsten core is mainly responsible for jacketed rod performance, not the homogenized properties.

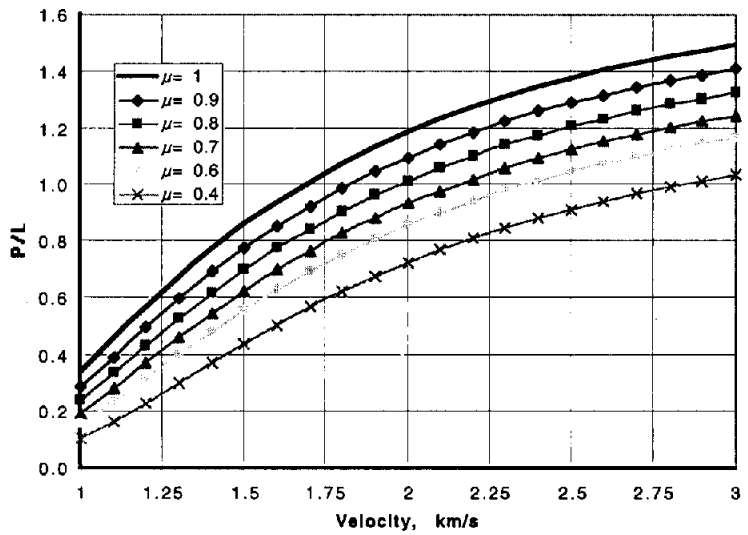

Fig. 6. Average density P/L functions.

DISCUSSION

AUTODYN simulations did not correctly predict the absolute penetration seen in the experiments. Penetration depth was underestimated by approximately 20-30% for each of the projectile configurations tested. Since the code was used in a predictive mode, there were no adjustments of parameters to match the all-tungsten baseline. However, the relative penetration of jacketed and unjacketed rods was more accurately predicted. The code predicts a ratio of 0.91 between $\mu = 0.6$ and $\mu = 1$; we measured 1.02.

The average density penetration function also did not compare well with the experiments. The penetration functions developed always under-predicted what was seen in the experiments. This could be partially attributed to the tungsten baseline test penetration being higher than predicted at 2.2 km/s by the Hohler and Stilp data. This effect is not enough to account for the discrepancy, and even had the tungsten penetration been the same in the model as the test, the model still predicts penetration should decrease when jackets are substituted for tungsten. This is contrary to the experimental results.

The shapes of the craters formed by the jacketed penetrators in the experiments indicate that, contrary to the AUTODYN simulations, the rod was not penetrating homogeneously. The first half of the penetration channel had a larger diameter than the second half. This occurred in all three of the tests, and an example of it can be seen in Figure 7. The figure shows a radiograph of the second target plate and a photo of a section through both target plates. It is hypothesized that the tungsten and steel formed the larger diameter portion of the crater, while only the tungsten core formed the narrow diameter portion. This would imply that the steel eroded at a faster rate than the tungsten and did not create a stable penetration front with the eroding tungsten. The core appeared to outrun the jacket during the penetration event.

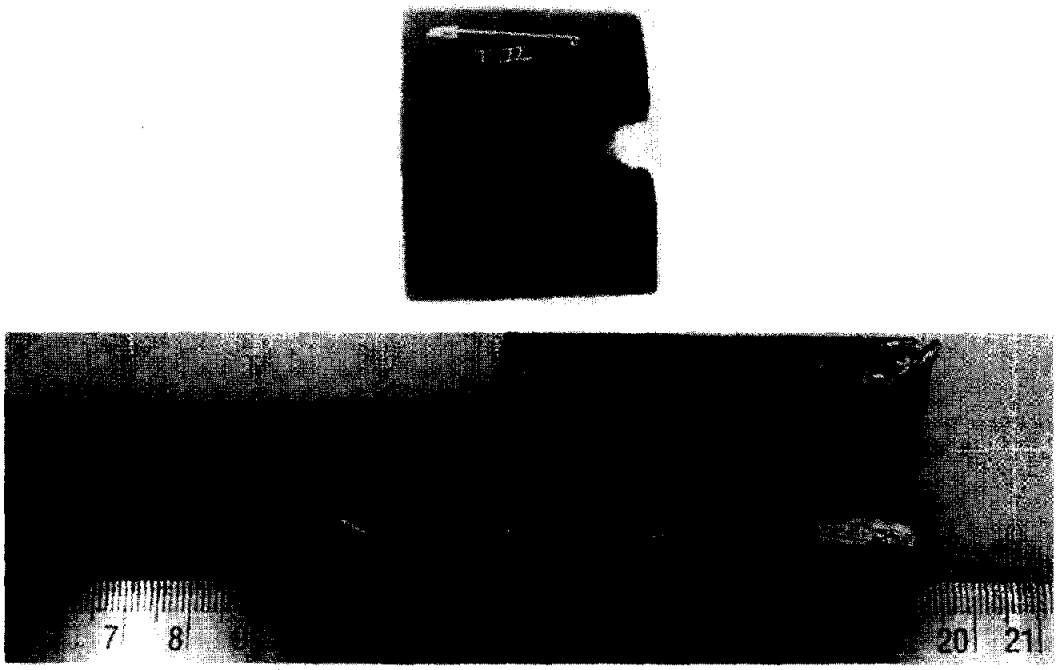

Fig. 7. Radiograph and photo of sectioned target.

Orphal, *et al.* [7] discusses "bi-erosion" and "co-erosion" penetration modes of jacketed rods. Bi-erosion denotes the penetration mode in which the core and jacket penetrate at different rates. Bi-erosion is hypothesized to occur when the jacket does not fit within the cavity diameter. Co-erosion is the condition when the jacket fits inside the tungsten mushroom head and both are penetrating together in a stable penetration front. Lee [8] proposed a criteria for determining whether jacketed rods penetrate in a bi-erosion or co-erosion mode. We applied his model to steel-jacketed tungsten impacting RHA at 2.2 km/s. That model predicts that for $\mu > 0.24$, the penetration mode should be co-erosion. This is contrary to all of the present results. However, consistent with Lee, in our tests the initial cavity diameter was always large enough to accommodate the jacket. Thus, the triggering event for bi-erosion must be different from what Lee assumed.

Depth measurements were made for both the wide and narrow portions of the penetration channel. A graphical representation that shows a comparison of the actual and the predicted steel and tungsten penetration results can be seen in Figure 8. The figure shows the actual penetration depths as measured from the experiments and the depths predicted by Hohler and Stilp [6] L/D=10 tungsten and steel penetration functions. It was assumed that the larger diameter portion of the crater was the steel's contribution to the total penetration, while the tungsten contributed to the total depth. The expected penetration of steel from the Hohler and Stilp data agrees quite well with the crater diameter transition depths (the interface between the wide and narrow portions of the crater) from the experiments. The penetration of the tungsten core, however, was underpredicted for the all-tungsten rod and the μ=0.6 jacket case using the function shown in Figure 5. The μ=0.4 jacket did not perform as well the all-tungsten rod. Also shown in the figure for each of the tests is the jacketed penetrator average density penetration model as compared to the experimental results. This clearly shows that the average density model is not correct for predicting jacketed rod penetration. Most significantly, comparing the tungsten penetration depths show that using a relatively thick, steel jacketed L/D=10 rod causes no penetration degradation against RHA targets.

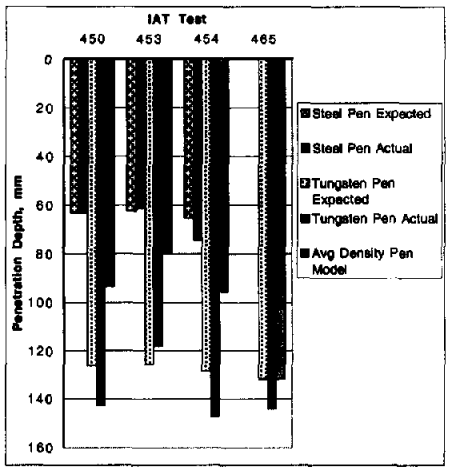

Fig. 8. Comparison of predicted and actual penetration depths.

Figure 9 shows penetrator efficiency ($P/KE^{1/3}$) as a function of diameter ratio (μ) for the AUTODYN simulations and the IAT experimental data. As can be seen in the Figure, the IAT test data for jacketed rods of μ=0.6 show a far greater efficiency as compared to the tungsten rod test (μ=1). The improvement is 21% for the μ=0.6 jackets and about 6% for the μ=0.4 jackets. Therefore, steel jackets appear to be a remarkably effective way to improve performance of hypervelocity tungsten rods. If the improvements observed here hold true for higher L/D ratios, the implications for the design of hypervelocity penetrators are startling.

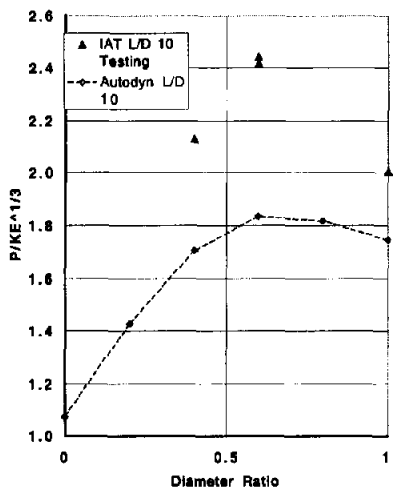

Fig. 9. Penetration efficiency of jacketed penetrators.

CONCLUSIONS

Steel jacketed tungsten penetrators were tested and were found to significantly improve the penetration efficiency as compared to baseline tungsten alloy rods. For a core-to-jacket diameter ratio of 0.6, the penetration efficiency increased by 21%. This was achieved because there was no apparent penetration degradation for adding a steel jacket. Experiments and AUTODYN simulations both showed the same penetration efficiency trends, but only the experiments showed the tungsten core outrunning the jacket.

Acknowledgement—This work was supported by the U.S. Army Research Laboratory (ARL) under contract DAAA21-93-C-0101.

REFERENCES

[1] Sorensen B, Kimsey K, Zukas J, Frank K. Numerical analysis and modeling of jacketed rod penetration. *International Journal of Impact Engineering*, 1999; **22**: 71-91.

[2] Lehr H, Wollman E, Koerber G. Experiments with jacketed rods of high fineness ratios. *International Journal of Impact Engineering*, 1995; **17**: 517-526.

[3] Lanz W, Lehr H. Craters caused by jacketed heavy metal projectiles of very high aspect ratios impacting steel targets. *16th International Symposium on Ballistics*, San Francisco, CA, 1996.

[4] Bjerke T, Silsby G, Scheffler D, Mudd P. Yawed long-rod armor penetration. *International Journal of Impact Engineering*, 1992; **12**: 281-292.

[5] Lanz W, Odermatt W. Penetration limits of conventional large caliber anti-tank guns / kinetic energy projectiles. *13th International Symposium on Ballistics*, FOA, Sundyberg, Sweden, 1992.

[6] Hohler V, Stilp A, as referenced by Anderson C, Morris B, Littlefield D. Penetration mechanics database. *Southwest Research Institute*, San Antonio, TX, 1993.

[7] Orphal D, Miller C. Hypervelocity impact of high L/D penetrators. *Hypervelocity Impact Symposium*, 1986, DARPA-TIO-87-62, 1987.

[8] Lee M. Analysis of jacketed rod penetration. *International Journal of Impact Engineering*, 2000; **24**: 891-905.